JPEDAV (2004) 25:237-251
DOI: 10.1361/15477030419496
1547-7037/$19.00 ©ASM International

Interdiffusion in Multiphase, Al-Co-Cr-Ni-Ti Diffusion Couples

T. Gómez-Acebo, B. Navarcorena, and F. Castro

(Submitted 25 June 2003)

The interdiffusion in Co matrix/Al particle alloys and Co/Ni-based substrates was studied using electron probe microanalysis and was simulated with the software DICTRA. Alloys were prepared by mixing elemental powders and furnace melting under an inert atmosphere. The phases involved in the study were γ (Ni-based or Co-based), β-CoAl, and γ′. The alloys were single-phase (γ) as well as two-phase (γ + β and γ + γ′). Several equilibrium points in the Al-Co-Cr system were measured and compared with the calculated diagram at 1100 °C. The diffusion couples were prepared to produce combinations of selected alloys and were subjected to annealing at 1100 °C for times up to 72 h. The diffusion calculations made with DICTRA were performed using the TCNI1 thermodynamic database together with mobility data collected from different literature sources. A literature survey on diffusion data of this system was performed, and comparisons with available data were made. The validity of the selected mobility data was checked with the composition profiles measured on some single-phase γ/γ diffusion couples. In the γ + β/γ and γ/γ + γ′ diffusion couples, a regression of the dispersed phase (β or γ′) was observed due to the interdiffusion of Al. From combined experimental and theoretical results, the effects of temperature and coating thickness were determined as an input for a coating lifetime prediction model.

1. Introduction

Overlay coatings are generally applied to land-based combustion turbine blades to improve oxidation and corrosion resistance. Typical overlay coatings are so-called MCrAlY, where M is iron, nickel, and/or cobalt. The efficiency of these coatings diminishes with time after exposure to high temperatures. Lifetime estimations of overlay coatings in Ni-based superalloys require a careful modeling of the coating degradation. Several models have been published[1-4] that consider degradation due to the following three different phenomena: oxidation; interdiffusion; and oxide spallation. Spallation occurs in materials experiencing thermomechanical fatigue due to cyclic operation of the turbine. Oxidation of the coating forms a protective layer, provided that the Al content in the coating surface is higher than a critical value.[5] The oxide layer grows in conformity with a parabolic law. Interdiffusion between the coating and the substrate is enhanced at high temperatures. In the absence of spallation (i.e., in turbines operated in the steady state) the following two criteria have been proposed for defining the onset of coating failure: (a) a critical Al content[5]; and (b) the volume fraction of the β-phase.[4] Interdiffusion is the main factor of Al loss in the coating, which is higher than that produced by oxidation.

Computer simulations of multiphase materials can be used as an aid to estimate the lifetimes of coatings, provided that the thermodynamic and kinetic descriptions of the alloy system are well known. For Ni-base superalloys, there are good recent thermodynamic[6] and kinetic[7] descriptions. However, with Co as one of the main components of several MCrAlY coatings, the necessary modifications of the thermodynamic and kinetic descriptions of the Al-Co-Cr system are not fully known.

Morral et al.[8] have analyzed the different types of planar boundaries in multiphase diffusion couples. Three types of planar boundaries can exist. These are boundaries across which there are changes of zero phases (type 0), one phase (type 1), or two phases (type 2). Depending on the movement of the boundary, a shorthand notation for the couples was proposed.

In this work, interdiffusion experiments have been done at 1100 °C for several alloys in the Al-Co-Cr-Ni-Ti system. The results have been compared with calculations performed with Thermo-Calc[9] and DICTRA.[10] It has been shown that Al composition profiles are well reproduced, but the agreement is not so good for other elements such as Cr. Finally, a life estimation is done as a function of some operating parameters.

2. Materials and Experimental Procedure

Several alloys were prepared from elemental metals by mixing 20 g of the metallic powders in a Turbula shaker-mixer (Model T2C, Willy A. Bachofen AG Maschinenfabrik, Basel, Switzerland) for 30 min. Characteristics of the metallic powders are shown in Table 1. Nominal and measured compositions for the mixtures are given in Table 2. The powder mixtures were uniaxially pressed at 400 MPa. Compacts were introduced into Al_2O_3 crucibles and were

T. Gómez-Acebo, B. Navarcorena, and **F. Castro,** CEIT and University of Navarra, Manuel Lardizabal 15, E-20018 San Sebastian, Spain. Contact e-mail: tgacebo@ceit.es.
Paper presented at Calphad XXXII, La Malbaie, Québec, Canada, May 25-30, 2003.

Table 1 Characteristics of the Elemental Powders

Element	Purity (%)	Particle Size	Supplier	Impurities (ppm)
Al	99.5	400 μm maximum	Goodfellow	Cu < 200, Fe < 3500, Mn < 200, Si < 2500
Cr	99	200 μm maximum	Goodfellow	Al 1600, Cu 30, Fe 2500, Si 500, C 200, S 80
Co	99.7	1 μm mean	OMG Americas, Inc.	O 2800, C 760, S < 10, Ni 20, Fe 23, Cu 10, Zn < 1, Mn 4, Na < 10, Mg 3, Ca 2, Si < 10
Ni	99.5	250 μm maximum	Goodfellow	Co < 5000, Cu < 900, Fe < 1500, C < 600, S < 50, oxides 1600
Ti	99.5	150 μm maximum	Goodfellow	C < 100 Cl 1700, Fe 200, N < 100, O 1000

Table 2 Alloy Compositions

Alloy System	Alloy Number	Composition (wt.%)	Composition (at.%)	Used in Couple
Al-Co	A1	Co-4.0Al	Co-8.3Al	C1, C2
	A2	Co-8.3Al	Co-16.5Al	C3
	A3	Co-9.0Al	Co-17.8Al	C4
	A4	Co-10.0Al	Co-19.5Al	C5
Co-Cr	A5.1	Co-8.9Cr	Co-9.9Cr	C1
	A5.2	Co-11.0Cr	Co-12.3Cr	C3
	A6.1	Co-14.0Cr	Co-15.6Cr	C2
	A6.2	Co-17.0Cr	Co-18.8Cr	C4
	A7	Co-30.0Cr	Co-32.7Cr	C5
Al-Co-Cr	A8	Co-5.0Al-25.7Cr	Co-10.0Al-26.6Cr	C9
	A9	Co-6.0Al-27.9Cr	Co-11.8Al-28.5Cr	C10
	A10	Co-6.6Al-28.7Cr	Co-12.9Al-29.1Cr	C13
	A11	Co-7.7Al-32.0Cr	Co-14.8Al-32.0Cr	C11
Al-Co-Ni	A12	Ni-5.0Al-28.9Co	Ni-10.5Al-27.2Co	C6, C7
	A13.1	Ni-5.3Al-38.4Co	Ni-10.9Al-36.1Co	C8, C10, C11
	A13.2	Ni-6.5Al-40.8Co	Ni-13.2Al-37.8Co	C9
	A14	Ni-7.7Al-25.8Co	Ni-15.4Al-23.6Co	C6
	A15	Ni-10.0Al-21.6Co	Ni-19.5Al-19.3Co	C7
	A16	Ni-10.8Al-20.0Co	Ni-20.9Al-17.7Co	C8
Al-Cr-Ni-Ti	A18	Ni-1.4Al-5.5Cr-8.9Ti	Ni-2.9Al-5.9Cr-10.5Ti	C13

Table 3 Temperature and Time for the Diffusion Anneal in the Different Couples

Alloy System	Couple No.	Composition of Alloys Used (wt.%) (a)	Phases	*T* (°C)	Time (h)
Al-Co-Cr	C1	Co-4.0Al (A1)/Co-8.9Cr (A5.1)	γ/γ	1100	72
	C2	Co-4.0Al (A1)/Co-14.0Cr (A6.1)	γ/γ	1100	72
	C3	Co-8.3Al (A2)/Co-11.0Cr (A5.2)	γ + β/γ	1100	72
	C4	Co-9.0Al (A3)/Co-17.0Cr (A6.2)	γ + β/γ	1100	72
	C5	Co-10.0Al (A4)/Co-30.0Cr (A7)	γ + β/γ	1100	72
Al-Co-Ni	C6	Ni-5.0Al-28.9Co (A12)/Ni-7.7Al-25.8Co (A14)	γ/γ	1100	24
	C7	Ni-5.0Al-28.9Co (A12)/Ni-10.0Al-21.6Co (A15)	γ/γ + γ′	1100	48
	C8	Ni-5.3Al-38.4Co (A13.1)/Ni-10.8Al-20.0Co (A16)	γ/γ + γ′	1100	72
Al-Co-Cr-Ni	C9	Co-5.0Al-25.7Cr (A8)/Ni-6.5Al-40.8Co (A13.2)	γ + β/γ	1100	48
	C10	Co-6.0Al-27.9Cr (A9)/Ni-5.3Al-38.4Co (A13.1)	γ + β/γ	1100	48
	C11	Co-7.7Al-32.0Cr (A11)/Ni-5.3Al-38.4Co (A13.1)	γ + β/γ	1100	48
Al-Co-Cr-Ni-Ti	C13	Co-6.6Al-28.7Cr (A10)/Ni-1.4Al-5.5Cr-8.9Ti (A18)	γ + β/γ	1100	72

(a) Alloy number is in parentheses.

melted in a furnace with graphite heating elements under Ar at a temperature that was 200 °C higher than the liquidus temperature of the mixture. The alloys were then homogenized at 1100 °C for 3 h in Ar and were quenched in water. Sheets of 2 mm thickness were cut from the samples and were polished with 3 μm diamond paste. These samples

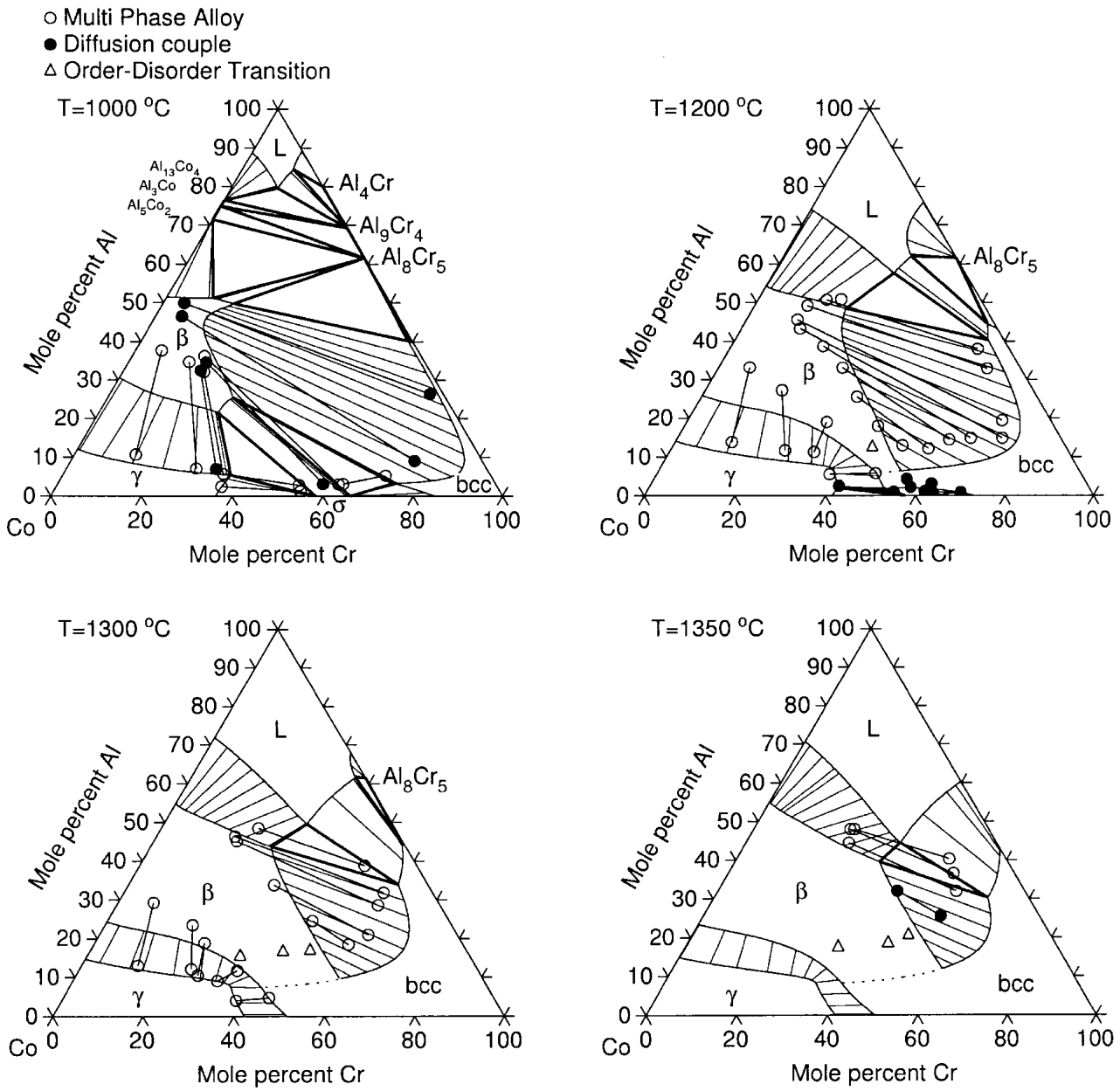

Fig. 1 Isothermal sections of the Al-Co-Cr system calculated with the TCNI1 database,[6] together with experimental data from Ishikawa et al.[11] at several temperatures

were studied using a scanning electron microscope (SEM) (model XL30, Philips, Amsterdam, The Netherlands) operating at a 20 kV acceleration voltage and were fitted with an energy dispersive x-ray microanalysis (EDS) system from EDAX (Mahwah, NJ). The samples also were studied by x-ray diffraction with an x-ray diffractometer (model PW1700, Philips).

The samples were then placed 2 by 2 facing each other and were joined in a hot-press furnace at 1100 °C and 35 MPa for 5 min under an Ar protective atmosphere. The interdiffusion due to this process was found to be negligible. These diffusion couples were consequently given a diffusion anneal in Ar at 1100 °C for different times, followed by water quenching. The diffusion couples that were produced are listed in Table 3.

The diffusion couples were cut into two halves and were prepared metalographically. The final polishing was done with 3 μm diamond paste. Semi-quantitative EDS analysis was performed along a line parallel to the diffusion interface, with manual spacing of 10 μm between the analyzed points. Measurements were performed as single line measurements for obtaining averaged compositional data in weight percent (wt.%). The terminal composition of the diffusion couples was measured at a distance far enough from the interface, where the composition did not change any longer. Some oxide particles that were present at the

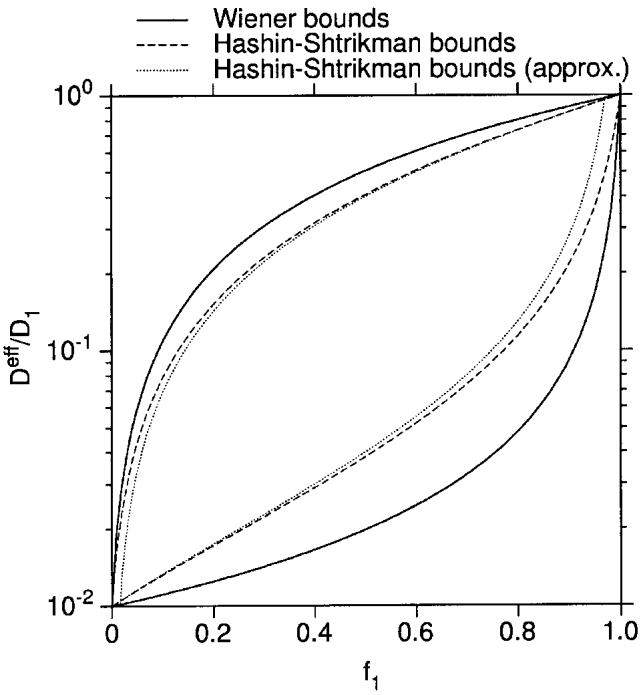

Fig. 2 Upper and lower bounds for the effective diffusivity in a two-phase system when $D_1 = 100\ D_2$: solid lines are upper ($D^{eff} = f_1D_1 + f_2D_2$) and lower [$D^{eff} = 1/(f_1/D_1 + f_2/D_2)$] Wiener bounds. Dashed lines are upper and lower H-S[22] bounds given by Eq 8 and 9, respectively. Dotted lines are the approximations given by Eq 10 and 11.

polished surface of the alloys were used as markers of the Kirkendall interface.

The impurities of the starting alloys did not form any compound with aluminum (Al), cobalt (Co), chromium (Cr), nickel (Ni), and titanium (Ti); no influence of these impurities was found in the diffusion profiles.

3. Calculation Procedure

3.1 Thermodynamic Description

The thermodynamic calculations have been performed with the TCNI1 database,[6] which includes an assessed description of all the binary systems involved in this work. It also includes completely assessed descriptions for the ternaries: Al-Co-Ni; Al-Cr-Ni; Al-Cr-Ti; Al-Ni-Ti; and Cr-Ni-Ti. There is no assessment for the remaining ternaries: Al-Co-Cr; Al-Co-Ti; Co-Cr-Ni; Co-Cr-Ti; and Co-Ni-Ti. All of these latter ternary systems contain Co in their composition.

Of the non-assessed ternaries, the Al-Co-Cr is of great importance for the study of the stability of high-temperature MCrAlY overlay coatings. There has been some experimental information about the phase relations in this system published by Ishikawa et al.[11] The reported experimental data are presented in Fig. 1, together with the calculated isothermal sections of the system. The calculation was done as an

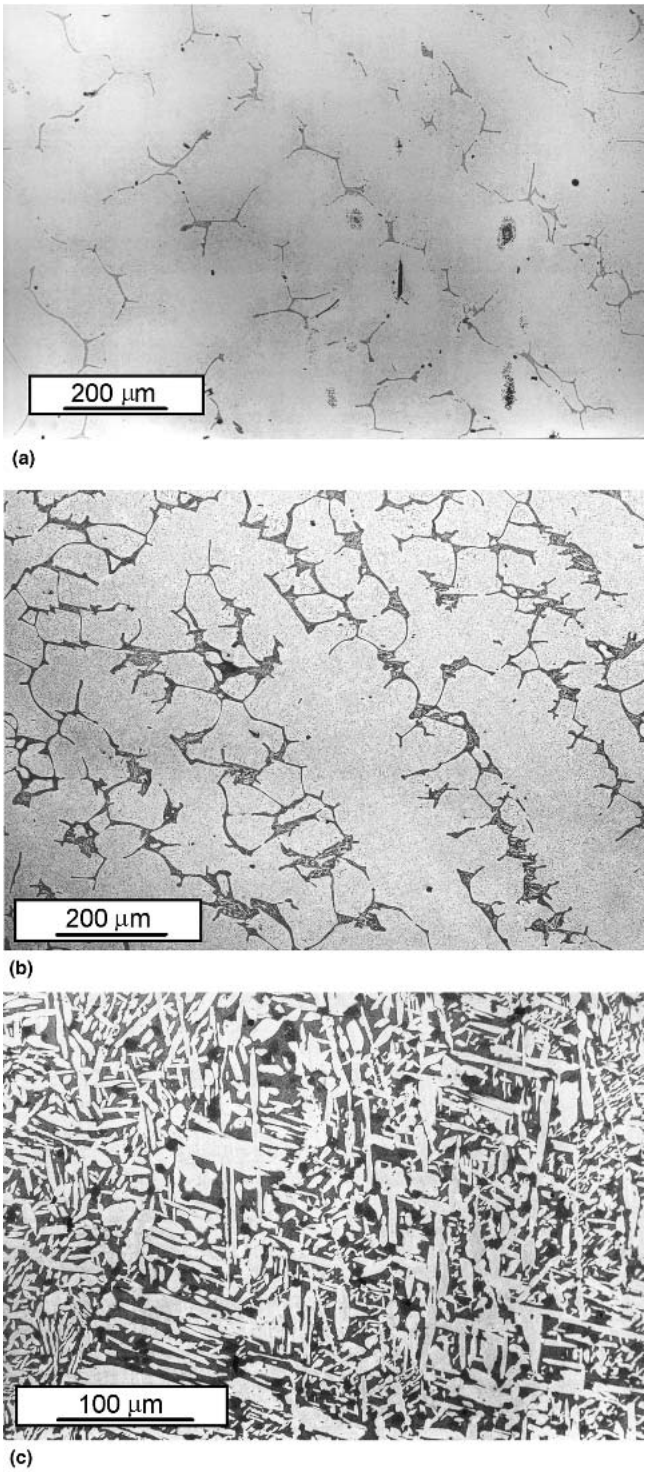

Fig. 3 SEM photomicrographs of the two-phase Al-Co-Cr alloys represented in Fig. 4. Chemical compositions in wt.%: (**a**) A8 (Co-5.0Al-25.7Cr); (**b**) A9 (Co-6.0Al-27.9Cr); and (**c**) A11 (Co-7.7Al-32.0Cr)

extrapolation from the three binaries, without any ternary interaction parameter. There is a reasonable agreement between the calculated diagram and the experimental data,

Table 4 Measured and Calculated Volume Fraction of the B2 Phase in the Al-Co-Cr Ternary Alloys

Alloy Number	Composition (wt.%)	Measured Volume Fraction of the B2 Phase	Calculated Mole Fraction of the B2 Phase
A8	Co-5.0Al-25.7Cr	0.06	0.03
A9	Co-6.0Al-27.9Cr	0.24	0.23
A11	Co-7.7Al-32.0Cr	0.59	0.51

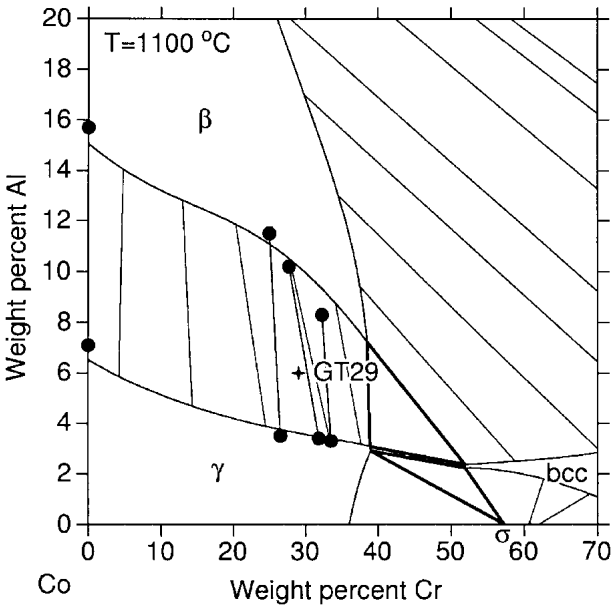

Fig. 4 Section of the calculated Al-Co-Cr system at 1100 °C, together with the measured compositions of the phases in this ternary system and in the binary Al-Co. The chemical composition of the GT29 overlay coating is also shown (chemical composition in wt.%: Co-6Al-29Cr-0.3Y, without Y).

except for the composition of the β-CoAl (B2) phase. It can be seen in Fig. 1 that the compositional trend toward the Al-Co side of the triangles seems to be at too high an Al content in the B2 phase. Noting that the binary Al-Co is well-characterized,[12,13] those experimental data in the ternary were regarded as inaccurate, and the thermodynamic modeling of the ternary was accepted as an ideal system.

3.2 Kinetic Description

3.2.1 Modeling of the Diffusion Coefficients. From the absolute reaction rate the mobility of an arbitrary species i may be expressed as

$$M_i = \frac{M_i^0}{RT}\exp\left(\frac{-Q_i}{RT}\right) \quad \text{(Eq 1)}$$

where M_i^0 represents the frequency factor and Q_i represents the activation enthalpy. This expression can be written as

$$M_i = \frac{1}{RT}\exp\left(\frac{-\Delta Q_i^*}{RT}\right) \quad \text{(Eq 2)}$$

where $\Delta Q_i^* \equiv Q_i - RT\ln(M_i^0)$. The tracer diffusion coefficient D_i^* is related directly to the mobility as

$$D_i^* = RTM_i \quad \text{(Eq 3)}$$

The chemical diffusivity is given by a more complex relation in which the concentration of one element n has been chosen as dependent on the others. The chemical diffusivity $\tilde{D}_{ij}^n$ can be expressed as[14]

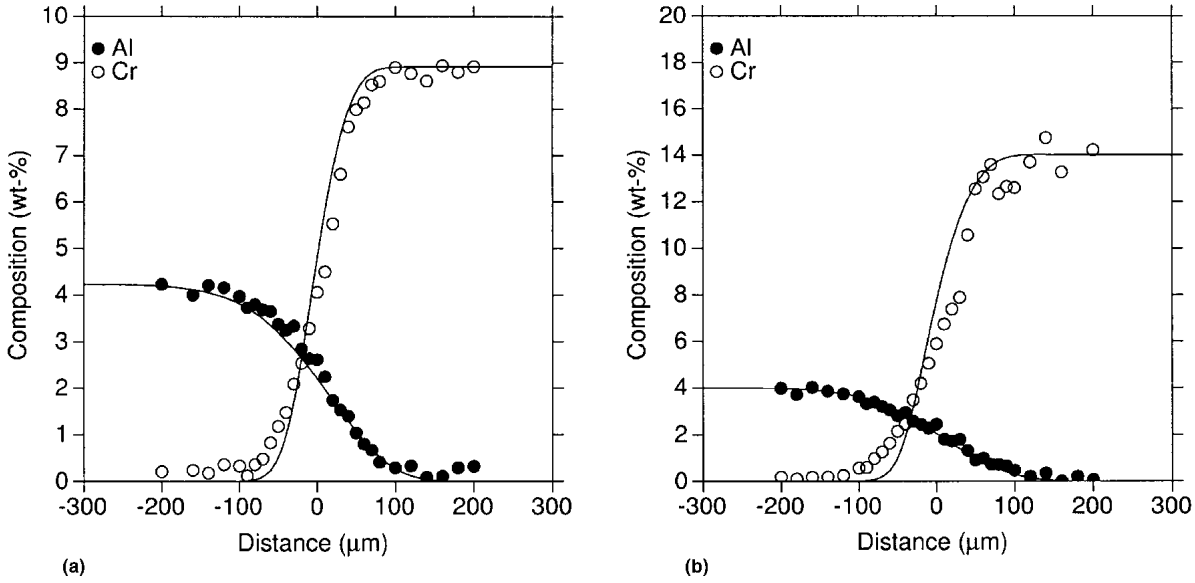

Fig. 5 Experimental and calculated composition profiles for Al and Cr of the diffusion couples (**a**) C1 and (**b**) C2, both annealed at 1100 °C for 72 h

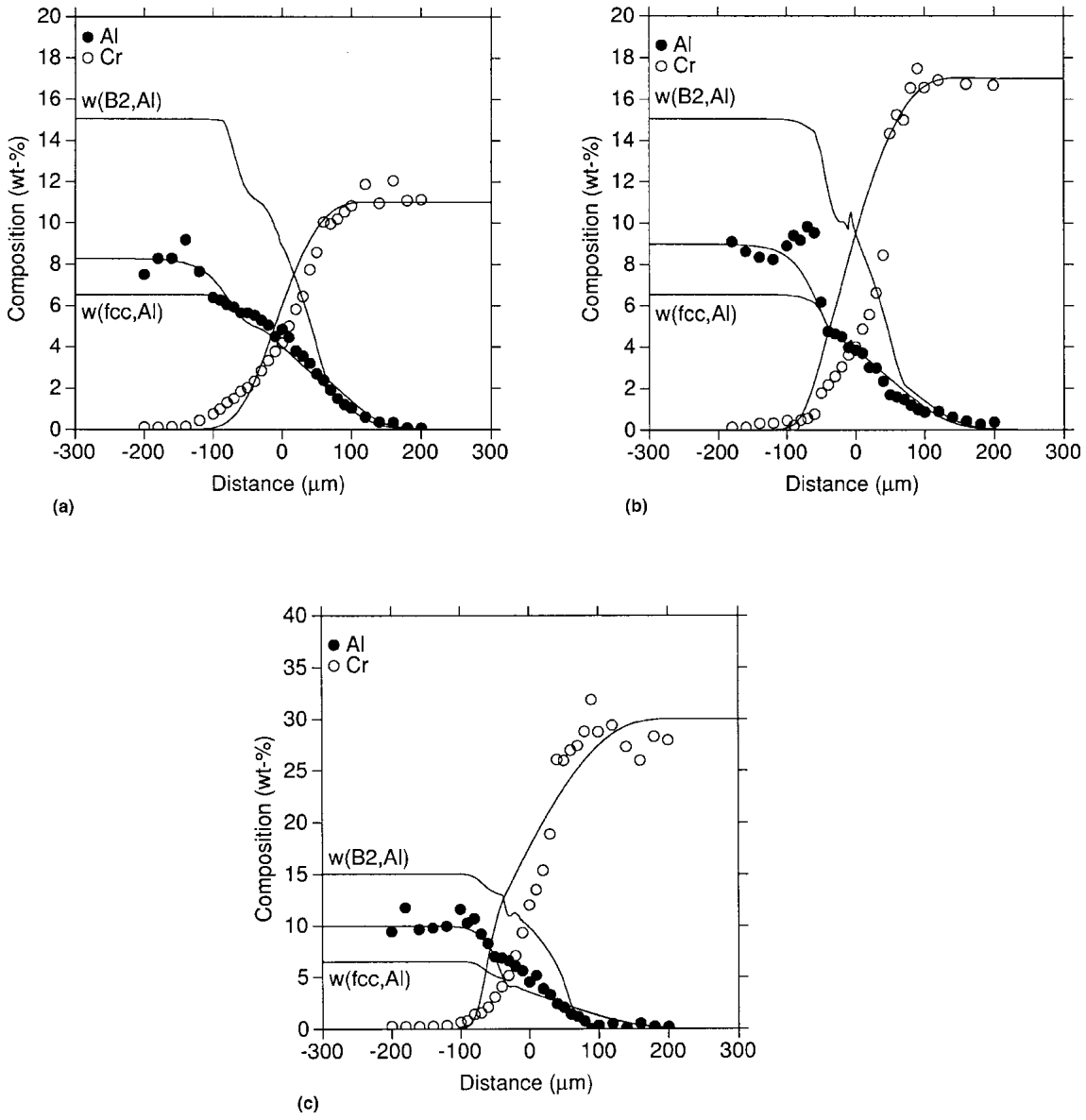

Fig. 6 Experimental and calculated composition profiles for Al and Cr of the diffusion couples (**a**) C3, (**b**) C4, and (**c**) C5, all annealed at 1100 °C for 72 h

$$\tilde{D}_{ij}^{n} = \sum_{k=1}^{n-1} (\delta_{ki} - x_i) x_k M_k \left(\frac{\partial \mu_k}{\partial x_j} - \frac{\partial \mu_k}{\partial x_n} \right) \quad \text{(Eq 4)}$$

where the Kronecker delta $\delta_{ki} = 1$ when $k = i$ and 0 otherwise, and x_k is the mole fraction of the element k. Using the chemical diffusivity, the flux of element k in the number-fixed frame of reference J_k can be calculated as

$$J_k = -\sum_{j=1}^{n} \tilde{D}_{kj}^{n} \frac{\partial c_j}{\partial z} \quad \text{(Eq 5)}$$

where $\partial c_j / \partial z$ is the concentration gradient of element j in the z direction.

The interactions in a multicomponent system can be modeled by means of the Redlich-Kister polynomials:

$$\Delta Q_i^* = \sum_j x_j Q_i^j + \sum_p \sum_{j>p} x_p x_j \sum_k {}^k A_i^{pj} (x_p - x_j)^k \quad \text{(Eq 6)}$$

where the Q_i^j and the ${}^k A_i^{pj}$ are linear functions of temperature, and are given in the Appendix. Only ${}^k A_i^{pj}$ parameters with $k = 0$ are used for this system. For example, in the ternary system Al-Co-Cr the term ΔQ_{Al}^* in Eq 2 is calculated as

$$\Delta Q_{Al}^* = x_{Al} Q_{Al}^{Al} + x_{Co} Q_{Al}^{Co} + x_{Cr} Q_{Al}^{Cr} + x_{Al} x_{Co} {}^0 A_{Al}^{Al,Co} + x_{Al} x_{Cr} {}^0 A_{Al}^{Al,Cr} + x_{Co} x_{Cr} {}^0 A_{Al}^{Co,Cr} \quad \text{(Eq 7)}$$

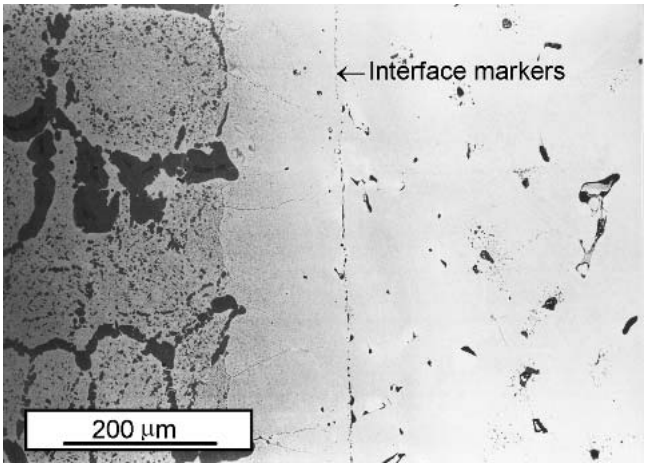

Fig. 7 SEM micrograph of the diffusion couple C4 annealed at 1100 °C for 72 h

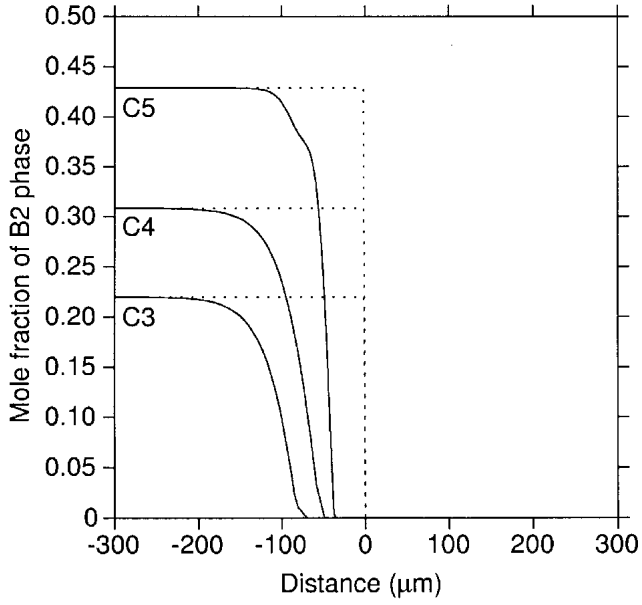

Fig. 8 Calculated regression of the β-phase in the diffusion couples C3, C4, and C5, all annealed at 1100 °C for 72 h

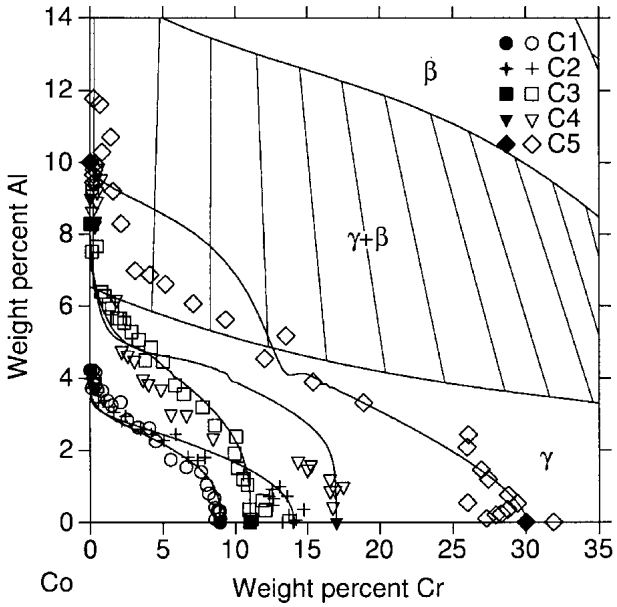

Fig. 9 Experimental and calculated diffusion paths of the Al-Co-Cr diffusion couples, together with the calculated isothermal section of the ternary phase diagram at 1100 °C

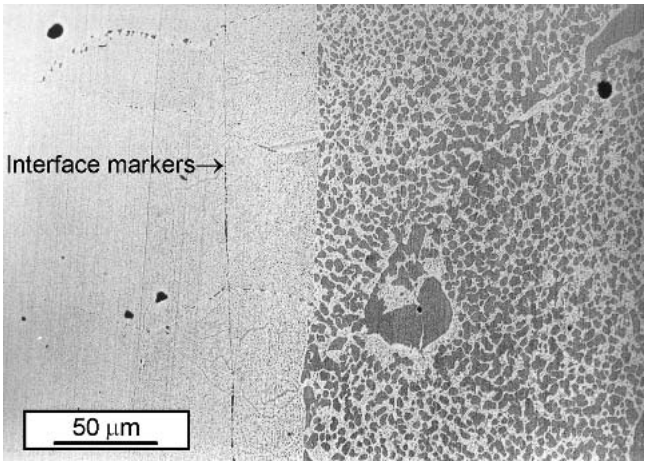

Fig. 10 SEM micrograph of the diffusion couple C7, annealed at 1100 °C for 48 h

3.2.2 Available Diffusivity Data. There are published assessments of the mobilities in the fcc phase for the following binary and ternary systems: Al-Cr[15]; Al-Ni[15]; Al-Ti[16]; Co-Ni[7]; Cr-Ni[17]; Ni-Ti[16]; Al-Cr-Ni[15]; and Al-Ni-Ti.[16] All of these data were included in the mobility database published by Campbell et al.[7] For the following binary systems there are no published assessed mobility data: Al-Co; Co-Cr; Co-Ti; and Cr-Ti.

Engström and Ågren[18] have suggested the following approximations for the mobilities in the fcc phase: $Q_{Al}^{Ti} = Q_{Al}^{Ni}$; $Q_{Co}^{Cr} = Q_{Ni}^{Cr}$; $Q_{Co}^{Ti} = Q_{Co}^{Co}$; $Q_{Cr}^{Ti} = Q_{Cr}^{Ni}$; $Q_{Ti}^{Al} = Q_{Ti}^{Co} = Q_{Ti}^{Ti} = Q_{Ti}^{Ni}$; and $Q_{Ti}^{Cr} = Q_{Al}^{Cr}$. Also, Campbell et al.[7] suggested the approach $Q_{Ni}^{Ti} = Q_{Ni}^{Ni}$. All of these approximations have been accepted.

For the mobilities in the binary Al-Co, no assessment has been published. Impurity diffusion of Co in fcc-Al was measured by Peterson and Rothman.[19] The impurity diffusion of Al in fcc-Co has not been directly measured. We have accepted the data suggested in the MOB2 database,[20] (i.e., five times the self-diffusivity of fcc-Fe).

The following ternaries have been regarded as ideal: Al-Co-Cr; Al-Co-Ni; Al-Co-Ti; Al-Cr-Ti; Co-Cr-Ni; Co-Cr-Ti; Co-Ni-Ti; and Cr-Ni-Ti.

All the mobility parameters used in this work are included in the Appendix.

3.2.3 Diffusion in Dispersed Phases. Engström[21] has suggested the use of the Hashin-Shtrikman[22] (H-S) bounds for the study of diffusion in dispersed systems. When there

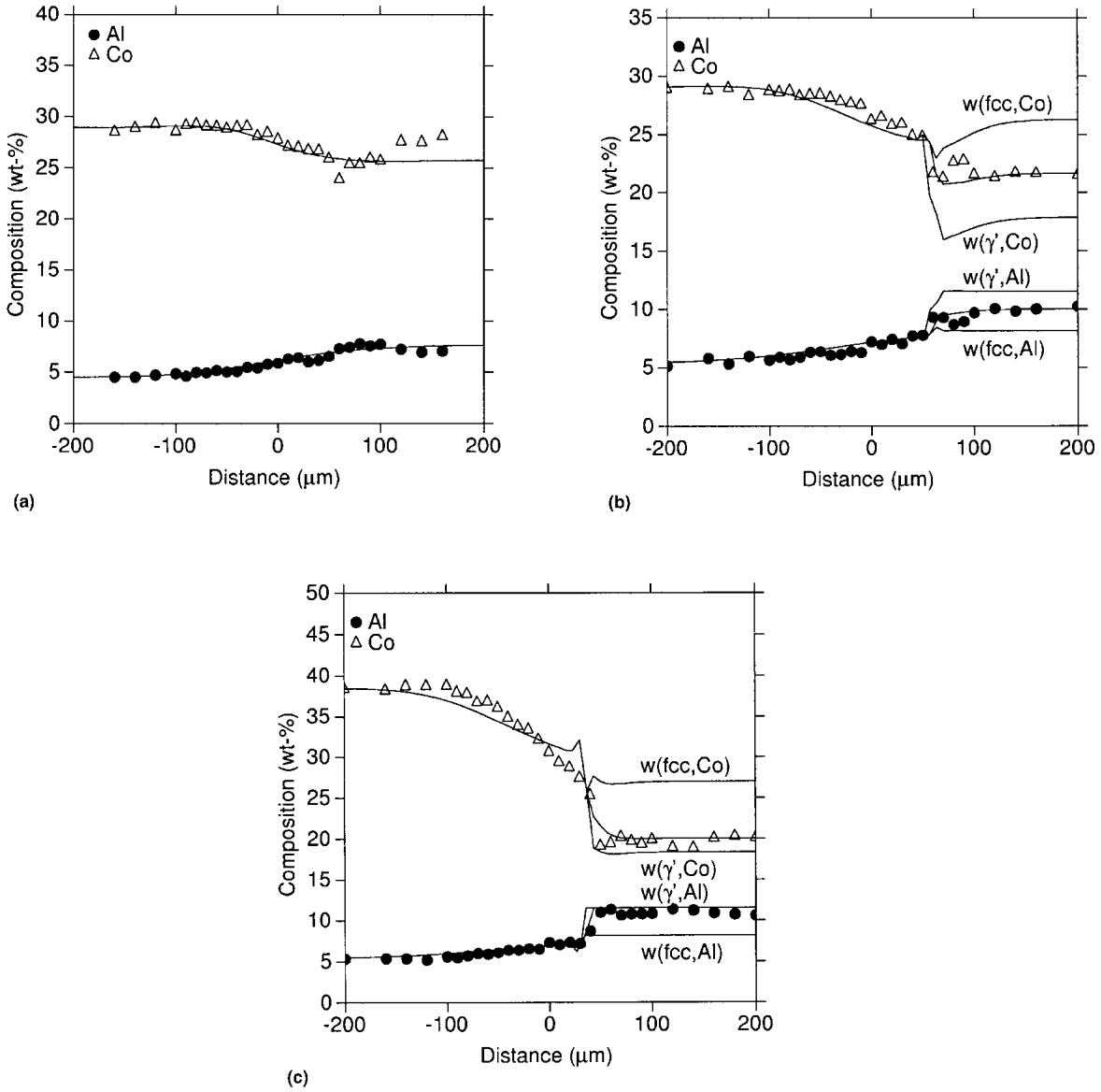

Fig. 11 Experimental and calculated composition profiles for Al and Co of the diffusion couples (**a**) C6, (**b**) C7, and (**c**) C8, all annealed at 1100 °C for 24, 48, and 72 h, respectively

is a big difference in the diffusivity of an element in two phases, say $D_\gamma > D_\beta$, the "effective" diffusivity in the two-phase $\gamma + \beta$ is reduced due to the presence of the β-phase. Upper and lower bounds to the effective diffusivity can be established.

Hashin and Shtrikman[22] used a variational principle to obtain bounds for the effective magnetic permeability of macroscopically homogeneous and isotropic mixtures of several phases. These bounds hold for any transport property such as the diffusion coefficient. For two-phase materials ($D_1 > D_2$), the upper D_u and lower D_l bounds are given by:

$$D_u = D_1 + \frac{f_2}{1/(D_2 - D_1) + f_1/(3D_1)} \quad \text{(Eq 8)}$$

$$D_l = D_2 + \frac{f_1}{1/(D_1 - D_2) + f_2/(3D_2)} \quad \text{(Eq 9)}$$

where f_i are the volume fractions, and D_i is the diffusivity within each phase. These bounds are widely accepted as the most restrictive ones, depending only on the volume fraction, and are otherwise independent of microgeometry. They are illustrated in Fig. 2 for the case when $D_1 = 100\ D_2$, together with the Wiener bounds (direct and inverse rules of mixtures).

When $D_1 >> D_2$ and $f_1 > f_2$, the H-S upper bound (Eq 8) can be simplified to:

$$D_u = D_1\left(\frac{2f_1}{3 - f_1}\right) \quad \text{(Eq 10)}$$

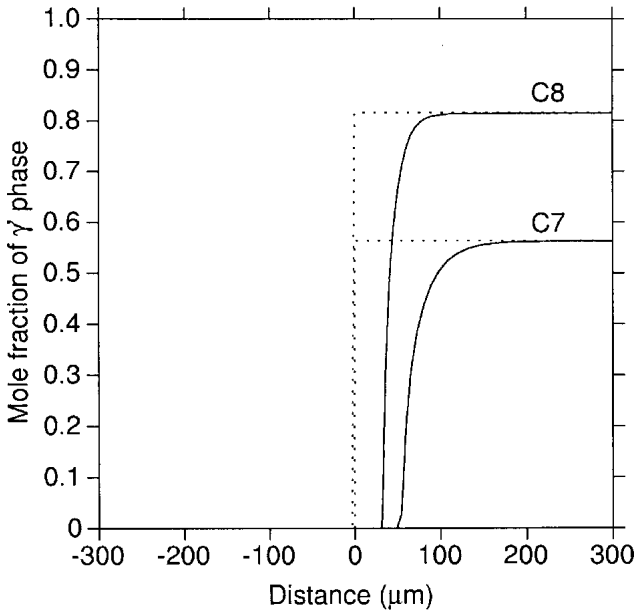

Fig. 12 Calculated regression of the γ′-phase in the diffusion couples C7 (1100 °C, 48 h) and C8 (1000 °C, 72 h)

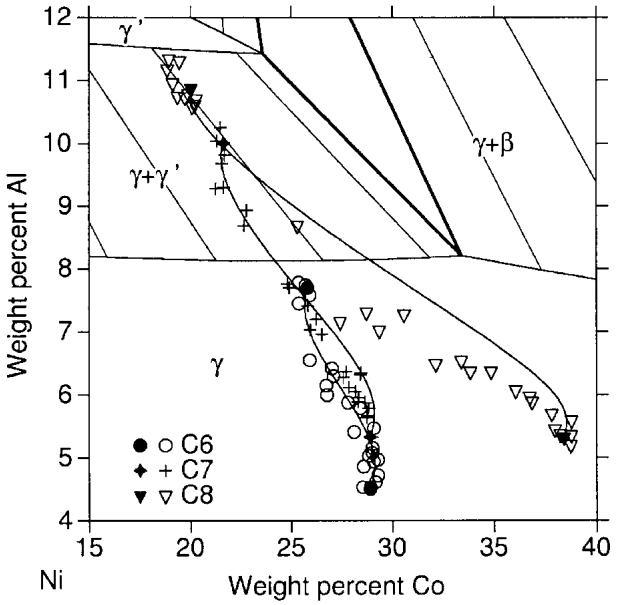

Fig. 13 Experimental and calculated diffusion paths of the Al-Co-Ni diffusion couples, together with the calculated isothermal section of the ternary phase diagram at 1100 °C

When $D_1 >> D_2$ and $f_1 < f_2$, the H-S lower bound (Eq 9) simplifies to:

$$D_1 = D_2\left(1 + 3\frac{f_1}{f_2}\right) \quad \text{(Eq 11)}$$

The terms in brackets in Eq 10 and 11 are the so-called labyrinth factors in the calculations. In this work, we have used the upper bound (Eq 10) for a correction of the diffusivity in the γ-phase due to the presence of the β-phase:

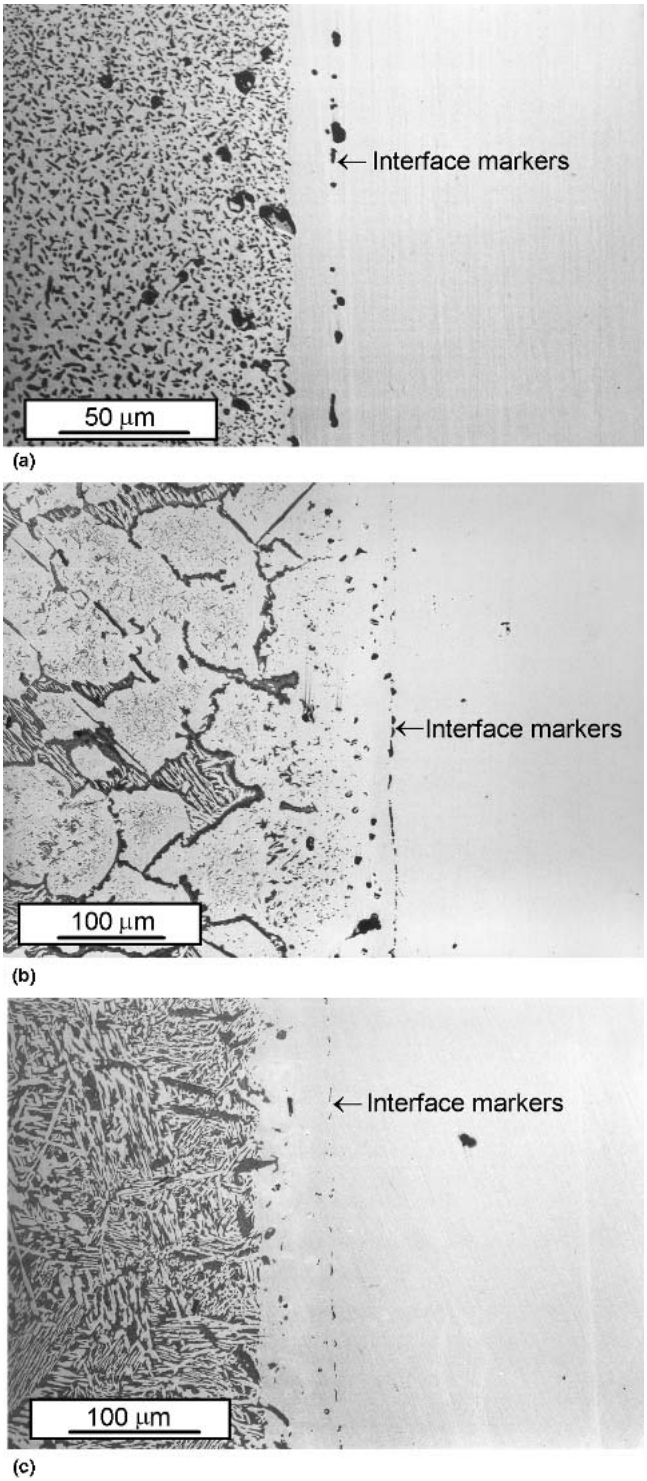

Fig. 14 SEM micrograph of the diffusion couples (**a**) C9, (**b**) C10, and (**c**) C11, all annealed at 1100 °C for 48 h. The cast microstructure of the left-hand alloys of the couples is shown in Fig. 3.

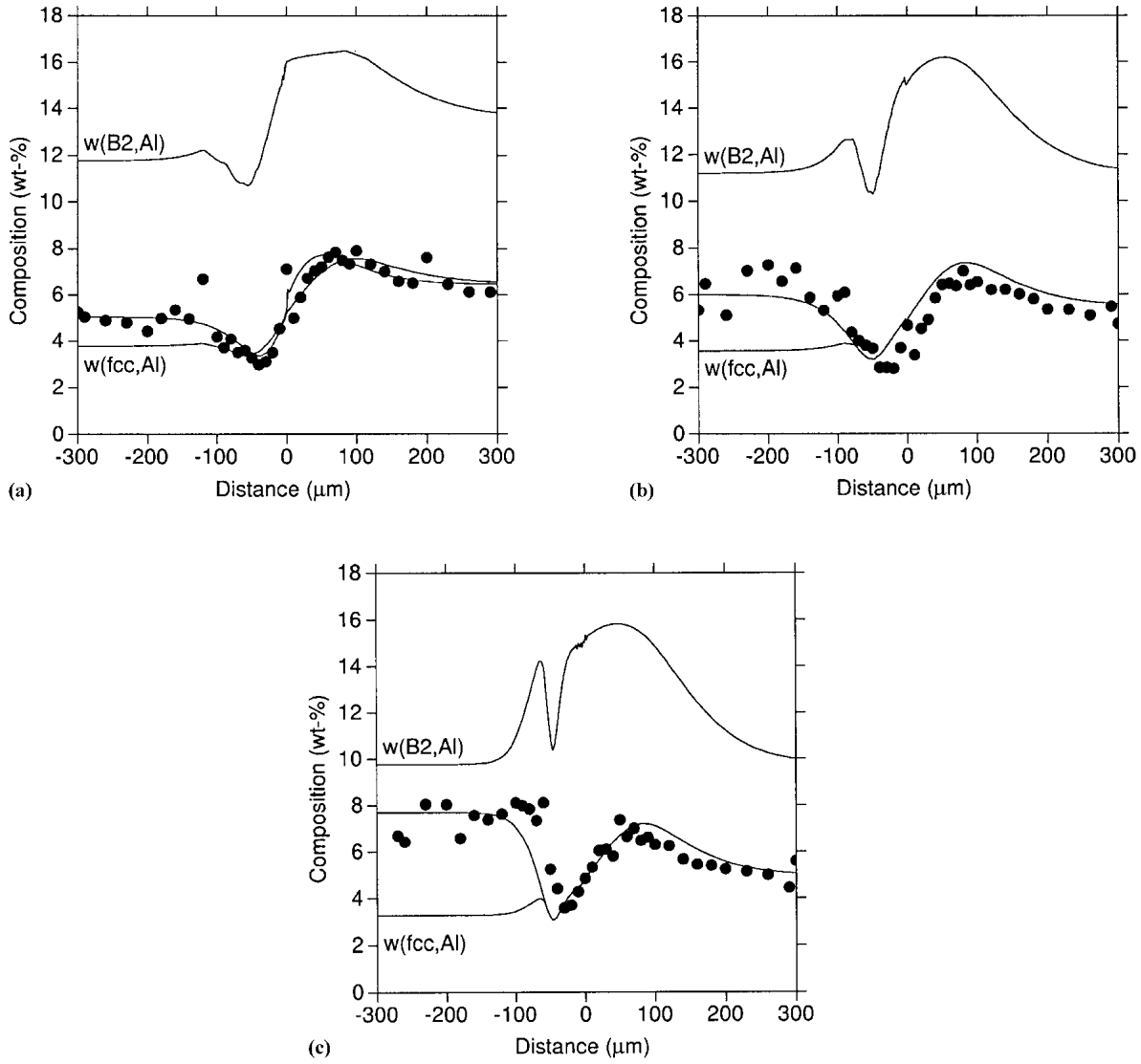

Fig. 15 Experimental and calculated composition profiles for Al of the diffusion couples (**a**) C9, (**b**) C10, and (**c**) C11, all annealed at 1100 °C for 48 h

$$D^{\text{eff}}/D_{\gamma} = \frac{2f_{\gamma}}{3 - f_{\gamma}} \qquad \text{(Eq 12)}$$

It has to be understood that this approach is an underestimate of the reduction of the diffusivity in the γ-phase, but, as a first approximation, it should be satisfactory.

4. Results and Discussion

4.1 Thermodynamics of the Al-Co-Cr System

Several ternary alloys in the Al-Co-Cr were produced, all of them being two-phase γ + β, with different volume fractions of the β-phase. The compositions of the alloys A8, A9, A10, and A11 are given in Table 2. SEM micrographs of these alloys are shown in Fig. 3. The matrix phase in all cases is the fcc γ-phase, while the β-phase (shown in dark contrast in the micrographs) is a dispersed phase. The measured and calculated volume fraction of the β-phase in three of these alloys is shown in Table 4. The agreement is good.

The compositions of the two phases are represented in Fig. 4, together with the calculated isothermal ternary section at 1100 °C. The agreement is also satisfactory, even though the calculation has been made directly from the three binary systems. Compared with the experimental data reported by Ishikawa et al.[11] (Fig. 1), we have not measured the high Al content in the β-phase that they report. Our measurements agree better with the thermodynamic calculations. This supports the use of the current thermodynamic description of the ternary Al-Co-Cr system, with no ternary interaction parameter, at least for the γ + β region.

4.2 Diffusion Couples

The composition of the diffusion couples studied is presented in Table 3. The calculated diffusion profiles, together

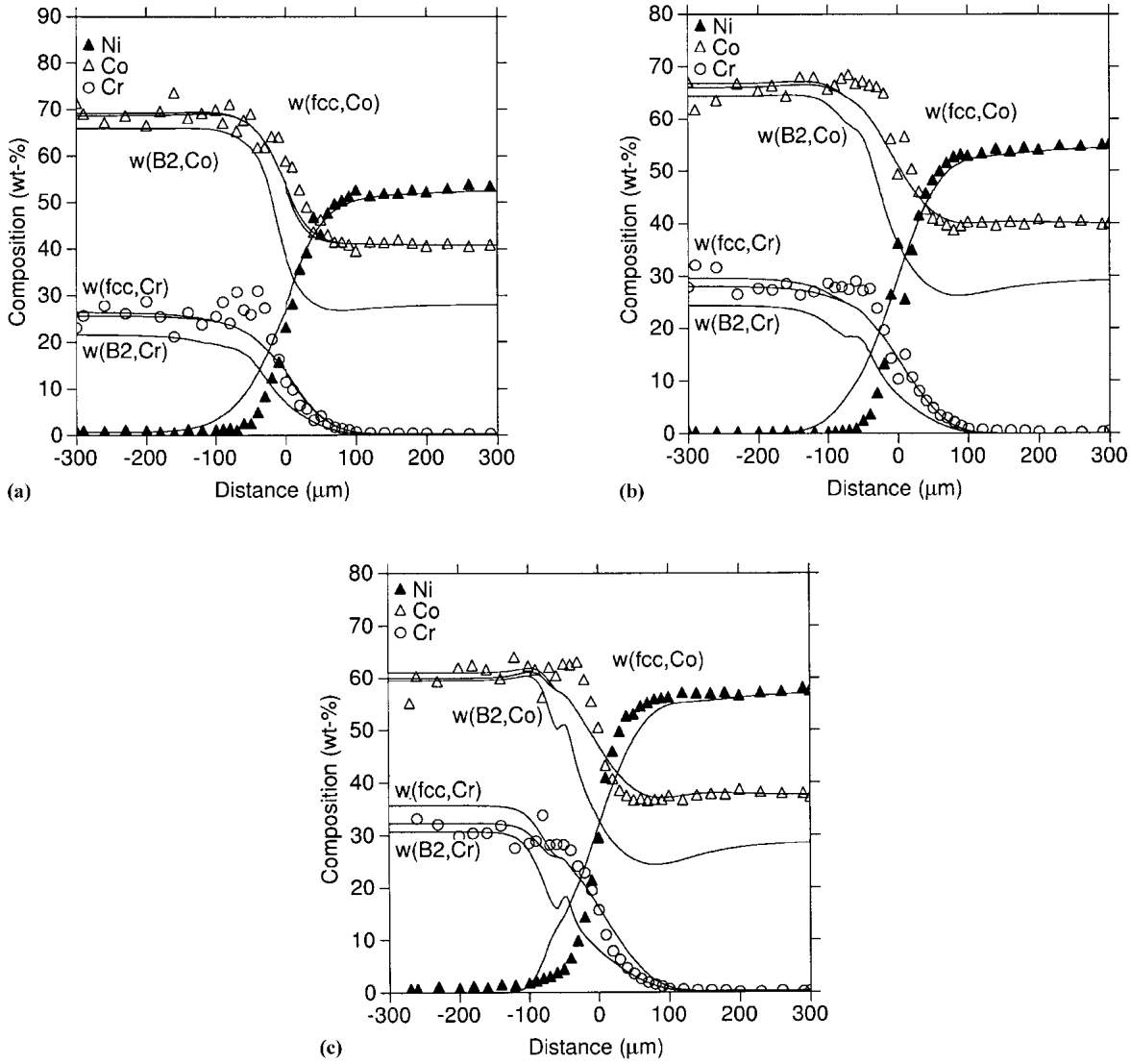

Fig. 16 Experimental and calculated composition profiles for Co, Cr and Ni of the diffusion couples (**a**) C9, (**b**) C10, and (**c**) C11, all annealed at 1100 °C for 48 h

with the measured chemical analyses using EDS, are shown in each section for several diffusion couples, distributed into the different chemical systems. Also the microstructures of some couples are shown.

4.2.1 Diffusion Couples in the Al-Co-Cr System

4.2.1.1 γ/γ Diffusion Couples. As a first check of the available mobility data, single-phase Al-Co γ alloys were subjected to diffusion with single-phase γ Co-Cr alloys. The Al and Cr diffusion profiles for diffusion couples C1 and C2 are shown in Fig. 5, together with the calculated profiles. The agreement for Al is very good, although for Cr it can be seen that the calculated mobilities are slightly underestimated.

4.2.1.2 γ + β/γ Diffusion Couples. Al-Co alloys with higher Al content are two-phase (γ + β) systems. Three different Al-Co alloys (γ + β) with increasing Al content were subjected to diffusion anneal with Co-Cr alloys (single-phase γ). The initial volume fraction of the β-phase in the Al-Co alloys varied from 0.22-0.42. Measured and calculated composition profiles for the diffusion couples are represented in Fig. 6. The calculations were made considering a reduced diffusivity in the γ + β-phase by the use of the labyrinth factor given in Eq 12. The Al calculated profiles shown in Fig. 6 include the following three different curves: the calculated average composition (intermediate line); and the phase composition in γ (fcc) and β (B2). These lines are drawn in the whole distance profile, although they are an extrapolation in the areas where the material is γ single phase. As in the γ/γ diffusion couples, the Al profiles are very well-predicted, but the Cr profile is again underestimated. The measured Al profiles, although they are from semi-quantitative EDS analysis, suggest a slight peak in composition on the two-phase side (left side) of the diffusion couples, however, the simulations with DICTRA did not predict this peak.

In Fig. 7, the microstructure of one of these diffusion couples is shown. It can be clearly seen that, due to Al

interdiffusion, there is a regression in the β-phase. For the couple shown in the micrograph (C4), the regression is about 110 μm. The calculated mole fraction of this β-phase is shown in Fig. 8 for the three diffusion couples studied.

These diffusion couples can be expressed in shorthand notation proposed by Morral et al.[8] as

$$\gamma + \beta < \gamma$$

in which < indicates the direction of motion of the boundary between the two regions relative to the initial interface. They are boundaries of type 1, in which one phase is added or subtracted on crossing the boundary.

The diffusion paths for the five couples are shown in Fig. 9, with the calculated phase diagram of the Al-Co-Cr system at 1100 °C.

4.2.2 Diffusion Couples in the Al-Co-Ni System. Several alloys in the ternary system Al-Co-Ni, both single-phase and two-phase (γ + γ′), were prepared. The Al content in the γ + γ′ alloys was varied to change the volume fraction of the γ′-phase. The diffusion couples prepared were γ/γ (C6) and γ/γ + γ′ (C7 and C8). In Fig. 10, a micrograph of the C7 diffusion couple after annealing treatment is shown. The experimental diffusion profiles of Al and Co are shown in Fig. 11, together with the calculated profiles.

The diffusion couples tested in the Al-Co-Ni system are of type 1:

$$\gamma > \gamma + \gamma'$$

As in the γ + β/γ diffusion couples, there is a regression of the two-phase region due to Al interdiffusion. It is shown in Fig. 12 for the couples C7 (at around 70 μm) and C8 (35 μm).

The diffusion paths for these three couples are shown in Fig. 13, with the calculated phase diagram of the Al-Co-Ni system at 1100 °C.

4.2.3 Diffusion Couples in the Al-Co-Cr-Ni System. The diffusion couples C9, C10, and C11 were prepared by diffusion annealing of γ + β Al-Co-Cr alloys and γ Al-Co-Ni alloys. The Al-Co-Cr alloys were selected with compositions similar to a typical commercial overlay coating (GT29: Co-6Al-29Cr-0.5Y, nominal composition in wt.%), but without yttrium additions. The compositions of these alloys are represented in the ternary Al-Co-Cr phase diagram (Fig. 4) together with that of the GT29 alloy. The microstructure of these alloys is shown in Fig. 3.

The microstructure of the diffusion couples after the diffusion anneal is shown in Fig. 14. The dark phase is the intermetallic β-phase. In all cases, a regression of the β-phase is observed due to interdiffusion: about 20 μm in diffusion couple C9, 40 μm in C10, and 60 μm in C11. The measured diffusion profiles are shown in Fig. 15 (for Al) and Fig. 16 (for Co, Cr, and Ni), together with the calculated profiles. For Al and Cr, a good fit is observed in all cases, and also for Co and Ni in the single-phase region. However, the diffusion profiles of these elements are overestimated in the two-phase region. The calculated regression of the β-phase after 48 h of diffusion annealing at 1100 °C is shown in Fig. 17. For the diffusion couple C9 (with the lowest β-phase volume fraction), the calculation predicts the formation of a small region of β within the Ni-Al-Co alloy, with a type 0 interface. However, this could not be confirmed experimentally.

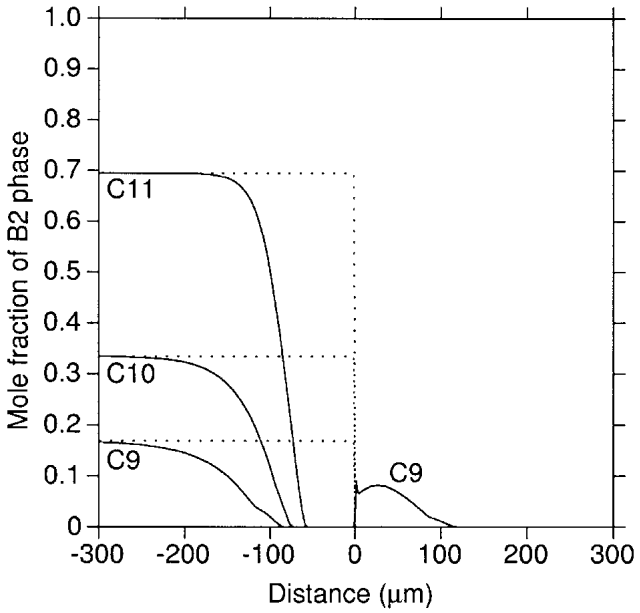

Fig. 17 Calculated regression of the β-phase in the diffusion couples C9, C10, and C11, annealed at 1100 °C for 48 h

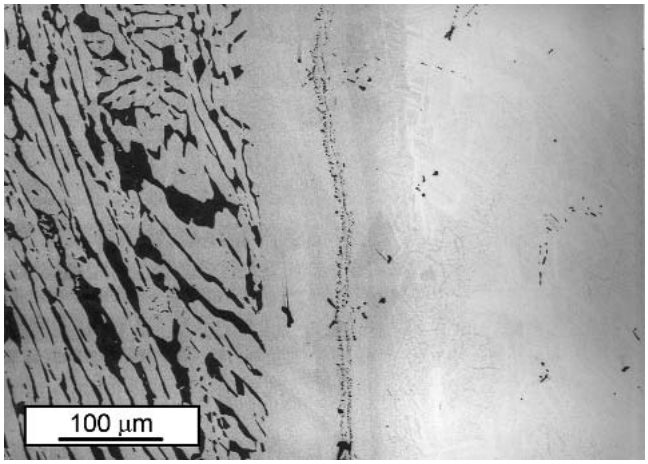

Fig. 18 SEM micrograph of the diffusion couple C13, annealed at 1100 °C for 72 h

4.2.4 Diffusion Couples in the Al-Co-Cr-Ni-Ti System. Finally, a two-phase γ + β Al-Co-Cr alloy of a composition similar to the overlay coating GT29 was subjected to diffusion annealing with a single-phase Cr-Ni-Ti alloy (diffusion couple C13). The microstructure of this diffusion couple is shown in Fig. 18. As in all the couples previously studied, there is a regression of the β-phase due to interdif-

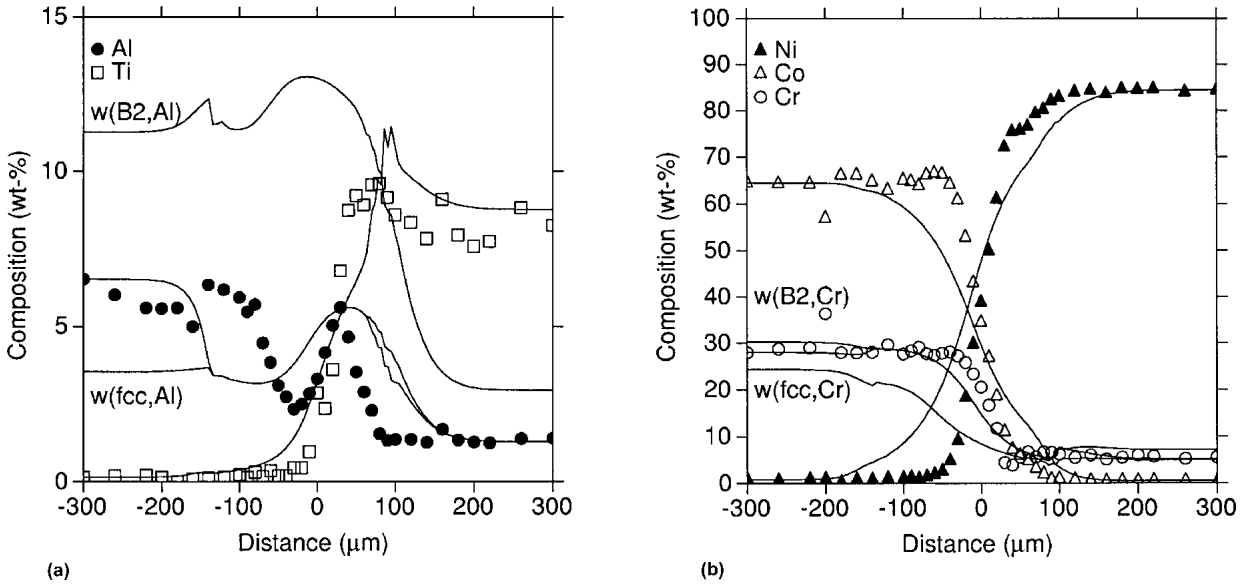

Fig. 19 Experimental and calculated composition profiles of the diffusion couple C13, annealed at 1100 °C for 72 h

fusion. The composition profiles are shown in Fig. 19 together with the calculated profiles. For Ni and Cr, the following three lines are represented: average calculated composition; and calculated composition of the two phases γ-fcc and β-bcc. Although there is some scatter in the measured compositions, the agreement with calculations is reasonably good, especially for Al. The diffusion of Ni is overestimated in the calculations. The calculated regression of the β-phase is shown in Fig. 20.

4.3 Life Assessment of MCrAlY Coatings

In land-operated gas turbines, interdiffusion between the coating and the substrate is more intensive at high temperatures. In the absence of spallation (i.e., in turbines operated in the steady state) the following two criteria have been proposed for defining the onset of coating failure: 1) a critical Al content in the surface[5]; and 2) depletion of the β-phase.[4] Interdiffusion is the main factor of Al loss in the coating, higher than that produced by oxidation.

While recognizing that diffusion of Cr and Ni in the diffusion couples that were examined is in some cases miscalculated with the current kinetic description, both the diffusion of Al and the regression of the β-phase are very well-predicted. This gives an opportunity for obtaining, at least, an estimate for the lifetime of the overlay coatings.

Lifetime estimations have been done using the criteria of the β-phase depletion in the coating. Oxidation has not been considered in this model, but it could be easily taken into consideration to refine the model. As a reference, the substrate studied has been the Ni-based superalloy GTD111 (chemical composition in wt.%: Ni-9.5Co-14Cr-3.0Al-3.8W-1.5Mo-4.9Ti-0.10C), but it has been simplified according to the available thermodynamic data in the TCNI1 database,[6] in which there is currently no information for Mo and C. This is a two-phase alloy (γ + γ′). The selected reference coating has been the GT29 overlay coating (chemical composition in wt.%: Co-29Cr-6Al-0.5Y), but it has been simplified by taking away yttrium from the calculations. This is a two-phase alloy (γ + β).

The calculations have been done supposing isothermal interdiffusion between an overlay coating of varying thickness (100-200 μm) with a substrate of 1 mm thickness. The onset of the coating has been supposed to be the time for depletion of the β-phase in the coating. Results are shown in Fig. 21. Such a figure can be used as an aid to the determination of the lifetime of a selected coating.

5. Conclusions

Several diffusion couples in the Al-Co-Cr-Ni-Ti system have been studied theoretically and experimentally at 1100 °C. Recently developed thermodynamic and kinetic databases of these systems have been used for the simulations. The system Al-Co-Cr has been especially reviewed, showing that the current thermodynamic description behaves reasonably well, at least for the γ + β region. The predicted diffusion profiles for Al show a very good fit to the experimentally measured compositions. For other elements such as Cr and Ni, the tendency is clearly predicted, although the current kinetic description cannot fit the experimental profiles. This suggests that a revision of these mobilities should be carried out.

Acknowledgments

The authors are grateful for funding of this work by the electrical company Iberdrola S.A. One of the authors (B.N.)

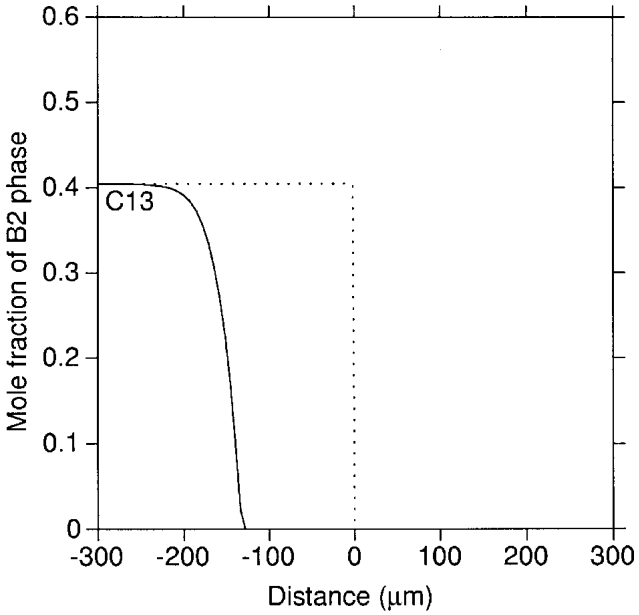

Fig. 20 Calculated regression of the β-phase in the diffusion couple C13, annealed at 1100 °C for 72 h

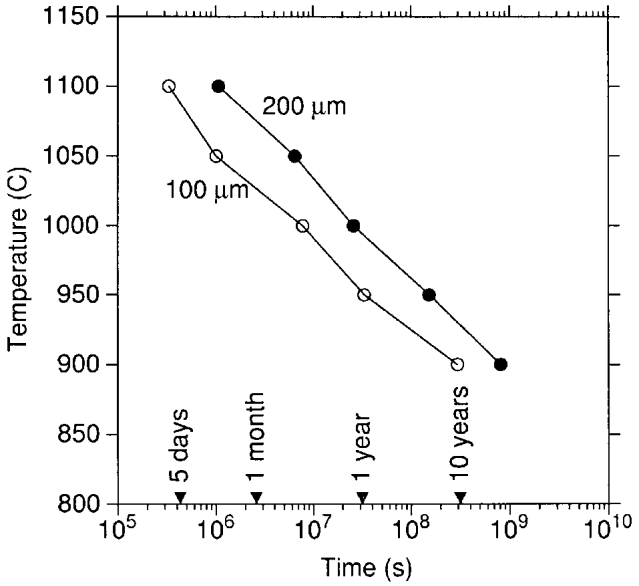

Fig. 21 Lifetime estimation of a GT29 overlay coating over a 1 mm Ni-based superalloy GTD111. Two different coating thicknesses are shown. Coating lifetime is calculated as the time for depletion of the B2 phase in the coating.

also acknowledges the Asociación de Amigos de la Universidad de Navarra for a research grant.

References

1. K.S. Chan, N.S. Cheruvu, and G.R. Leverant: "Coating Life Prediction for Combustion Turbine Blades," *J. Eng. Gas Turbines Power (Trans. ASME)*, 1999, *121*(3), pp. 484-88.
2. Y. Itoh and M. Tamura: "Reaction Diffusion Behaviors for Interface Between Ni-Based Super Alloys and Vacuum Plasma Sprayed MCrAlY Coatings," *J. Eng. Gas Turbines Power (Trans. ASME)*, 1999, *121*(3), pp. 476-83.
3. D.F. Susan and A.R. Marder: "Ni-Al Composite Coatings: Diffusion Analysis and Coating Lifetime Estimation," *Acta Mater.*, 2001, *49*(7), pp. 1153-63.
4. E.Y. Lee, D.M. Chartier, R.R. Biederman, and R.D.J. Sisson: "Modelling the Microstructural Evolution and Degradation of M-Cr-Al-Y Coatings During High Temperature Oxidation," *Surf. Coat. Technol.*, 1987, *32*, pp. 19-39.
5. J.A. Nesbitt and C.A. Barrett: "Predicting the Oxidation-Limited Lifetime of beta-NiAl" in *Proceedings of the First International Symposium on Structural Intermetallics*, R. Darolia, ed., Champion, PA, 1993, pp. 601-09.
6. N. Dupin and B. Sundman: "A Thermodynamic Database for Ni-Base Superalloys," *Scand. J. Metall.*, 2001, *30*(3), pp. 184-92.
7. C.E. Campbell, W.J. Boettinger, and U.R. Kattner: "Development of a Diffusion Mobility Database for Ni-Base Superalloys," *Acta Mater.*, 2002, *50*(4), pp. 775-92.
8. J.E. Morral, J. Cheng, A. Engström, and J. Ågren: "Three Types of Planar Boundaries in Multiphase Diffusion Couples," *Scr. Mater.*, 1996, *34*(11), pp. 1661-66.
9. B. Sundman, B. Jansson, and J.-O. Andersson: "Thermo-Calc Databank System," *Calphad*, 1985, *9*(2), pp. 153-90.
10. A. Borgenstam, A. Engström, L. Höglund, and J. Ågren: "DICTRA, A Tool for Simulation of Diffusional Transformations in Alloys," *J. Phase Equilibria*, 2000, *21*(3), pp. 269-80.
11. K. Ishikawa, M. Ise, I. Ohnuma, R. Kainuma, and K. Ishida: "Phase Equilibria and Stability of the BCC Aluminide in the Co-Cr-Al System," *Ber. Buns./Phys. Chem.*, 1998, *102*(9), pp. 1206-10.
12. N. Dupin: "Contribution à l'évaluation Thermodynamique des Alliages Polyconstitués à Base de Nickel," Ph.D. Thesis, Institut Nationale Polytechnique de Grenoble, France, 1995.
13. N. Dupin and I. Ansara: "Thermodynamic Assessment of the Al-Co System," *Rev. Metal.*, 1998, *95*(9), pp. 1121-29.
14. J.-O. Andersson and J. Ågren: "Models for Numerical Treatment of Multicomponent Diffusion in Simple Phases," *J. Appl. Phys.*, 1992, *72*(4), pp. 1350-55.
15. A. Engström and J. Ågren: "Assessment of Diffusional Mobilities in Face-Centered-Cubic Ni-Cr-Al Alloys," *Z. Metallkd.*, 1996, *87*(2), pp. 92-97.
16. N. Matan, H.M.A. Winand, P. Carter, M. Karunaratne, P.D. Bogdanoff, and R.C. Reed: "A Coupled Thermodynamic/Kinetic Model for Diffusional Processes in Superalloys," *Acta Mater.*, 1998, *46*(13), pp. 4587-600.
17. B. Jönsson: "Assessment of the Mobilities of Cr, Fe and Ni in Binary fcc Cr-Fe and Cr-Ni Alloys", *Scand. J. Metall.*, 1995, *24*(1), pp. 21-27.
18. A. Engström and J. Ågren: "Simulation of Diffusion in Multicomponent and Multiphase Systems," *Defect Diffusion Forum*, 1997, *143-147*, pp. 677-82.
19. N.L. Peterson and S.J. Rothman: "Impurity Diffusion in Aluminum," *Phys. Rev. B*, 1970, *1*, pp. 3264-73.
20. A. Engström: *MOB2 Alloy Mobility Database*, Thermo-Calc Software, Stockholm, Sweden, 1999.
21. A. Engström: "Interdiffusion in Multiphase, Fe-Cr-Ni Diffusion Couples," *Scand. J. Metall.*, 1995, *24*(1), pp. 12-20.
22. Z. Hashin and S. Shtrikman: "A Variational Approach to the Theory of the Effective Magnetic Permeability of Multiphase Materials," *J. Appl. Phys.*, 1962, *33*(10), pp. 3125-31.

Appendix: Kinetic Parameters for the fcc Phase

All parameters are given in J mol^{-1}.

Mobility of Al

$Q_{Al}^{Al} = -142\,000 + RT\ln(1.71 \times 10^{-4})$[15]
$Q_{Al}^{Co} = -286\,000 + RT\ln(3.5 \times 10^{-4})$[20]
$Q_{Al}^{Cr} = -235\,000 - 82\,T$[15]
$Q_{Al}^{Ni} = -284\,000 + RT\ln(7.5 \times 10^{-4})$[15]
$Q_{Al}^{Ti} = Q_{Al}^{Ni}$ [18]
${}^{0}A_{Al}^{Al,Cr} = 335\,000$[15]
${}^{0}A_{Al}^{Al,Ni} = -41\,300 - 91.2\,T$[15]
${}^{0}A_{Al}^{Al,Ti} = 335\,000$[16]
${}^{0}A_{Al}^{Cr,Ni} = -53\,200$[15]
${}^{0}A_{Al}^{Ni,Ti} = -53\,200$[16]

Mobility of Co

$Q_{Co}^{Al} = -174\,800 + RT\ln(4.64 \times 10^{-2})$[19]
$Q_{Co}^{Co} = -286\,175 - 76.0\,T$[7]
$Q_{Co}^{Cr} = Q_{Ni}^{Cr}$ [18]
$Q_{Co}^{Ni} = -284\,169 - 67.6\,T$[7]
$Q_{Co}^{Ti} = Q_{Co}^{Co}$ [18]
${}^{0}A_{Co}^{Co,Ni} = 10\,787 - 11.5\,T$[7]

Mobility of Cr

$Q_{Cr}^{Al} = -261\,700 + RT\ln(0.64)$[15]
$Q_{Cr}^{Co} = -246\,904 - 110\,T$[7]
$Q_{Cr}^{Cr} = -235\,000 - 82.0\,T$[17]
$Q_{Cr}^{Ni} = -287\,000 - 64.4\,T$[17]
$Q_{Cr}^{Ti} = Q_{Cr}^{Ni}$ [18]
${}^{0}A_{Cr}^{Al,Cr} = 487\,000$[15]
${}^{0}A_{Cr}^{Al,Ni} = -118\,000$[15]
${}^{0}A_{Cr}^{Cr,Ni} = -68\,000$[17]

Mobility of Ni

$Q_{Ni}^{Al} = -145\,900 + RT\ln(4.4 \times 10^{-4})$[15]
$Q_{Ni}^{Co} = -270\,348 - 87.3\,T$[7]
$Q_{Ni}^{Cr} = -235\,000 - 82.0\,T$[17]
$Q_{Ni}^{Ni} = -287\,000 - 69.8\,T$[17]
$Q_{Ni}^{Ti} = Q_{Ni}^{Ni}$ [7]
${}^{0}A_{Ni}^{Al,Cr} = 211\,000$[15]
${}^{0}A_{Ni}^{Al,Ni} = -113\,000 + 65.5\,T$[15]
${}^{0}A_{Ni}^{Al,Ti} = 211\,000$[16]
${}^{0}A_{Ni}^{Co,Ni} = 7866 + 7.65\,T$[7]
${}^{0}A_{Ni}^{Cr,Ni} = -81\,000$[17]
${}^{0}A_{Ni}^{Ni,Ti} = -81\,000$[16]

Mobility of Ti

$Q_{Ti}^{Al} = Q_{Ti}^{Ni}$ [18]
$Q_{Ti}^{Co} = Q_{Ti}^{Ni}$ [18]
$Q_{Ti}^{Cr} = Q_{Al}^{Cr}$ [18]
$Q_{Ti}^{Ni} = -256\,900 + RT\ln(8.6 \times 10^{-5})$[18]
$Q_{Ti}^{Ti} = Q_{Ti}^{Ni}$ [18]
${}^{0}A_{Ti}^{Al,Ni} = -118\,000$[16]
${}^{0}A_{Ti}^{Al,Ti} = 487\,000$[16]
${}^{0}A_{Ti}^{Ni,Ti} = -68\,000$[16]